

# Polymer translocation into a fluidic channel through a nanopore

Kaifu Luo<sup>1,\*</sup> and Ralf Metzler<sup>2,†</sup>

<sup>1</sup>*CAS Key Laboratory of Soft Matter Chemistry,  
Department of Polymer Science and Engineering,*

*University of Science and Technology of China, Hefei, Anhui Province 230026, P. R. China*

<sup>2</sup>*Physics Department, Technical University of Munich, D-85748 Garching, Germany*

(Dated: October 29, 2018)

Using two dimensional Langevin dynamics simulations, we investigate the dynamics of polymer translocation into a fluidic channel with diameter  $R$  through a nanopore under a driving force  $F$ . Due to the crowding effect induced by the partially translocated monomers, the translocation dynamics is significantly altered in comparison to an unconfined environment, namely, we observe a nonuniversal dependence of the translocation time  $\tau$  on the chain length  $N$ .  $\tau$  initially decreases rapidly and then saturates with increasing  $R$ , and a dependence of the scaling exponent  $\alpha$  of  $\tau$  with  $N$  on the channel width  $R$  is observed. The otherwise inverse linear scaling of  $\tau$  with  $F$  breaks down and we observe a minimum of  $\alpha$  as a function of  $F$ . These behaviors are interpreted in terms of the waiting time of an individual segment passing through the pore during translocation.

PACS numbers: 87.15.A-, 87.15.H-

## I. INTRODUCTION

Polymer translocation through a nanopore has attracted broad interest because it is of fundamental relevance in polymer physics and is also related to many biological processes, such as DNA and RNA translocation across nuclear pores, protein transport through membrane channels, or viruses injecting their DNA into a cell. Due to its potentially revolutionary technological applications [1, 2], including rapid DNA sequencing, gene therapy and controlled drug delivery, a considerable number of recent experimental [3–25] and theoretical [25–71] studies have been devoted to this subject.

The average translocation time  $\tau$  as a function of the chain length  $N$  is an important measure of the underlying dynamics. Standard equilibrium Kramers analysis [72] of diffusion across an entropic barrier yields  $\tau \sim N^2$  for unbiased translocation and  $\tau \sim N$  for driven translocation (assuming friction to be independent of  $N$ ) [27, 30]. However, the quadratic scaling behavior for unbiased translocation cannot be correct for a self-avoiding polymer [42] because the translocation time would be shorter than the Rouse equilibration time of a self-avoiding polymer,  $\tau_R \sim N^{1+2\nu}$ , where the Flory exponent  $\nu = 0.588$  in 3D and  $\nu_{2D} = 0.75$  in 2D [73, 74]. This renders the concept of equilibrium entropy and the ensuing entropic barrier inappropriate for translocation dynamics. Chuang *et al.* [42] studied the translocation for both phantom and self-avoiding polymers by numerical simulations with Rouse dynamics for a 2D lattice model and showed that for large  $N$ ,  $\tau \sim N^{1+2\nu}$ , the same scaling behavior as the equilibration time but with a much larger prefactor. This

result was recently corroborated by extensive numerical simulations based on the Fluctuating Bond (FB) [47] and Langevin Dynamics (LD) models with the bead-spring approach [49, 67].

For driven translocation, Kantor and Kardar [43] demonstrated that the assumption of equilibrium in polymer dynamics breaks down even more easily and provided a lower bound  $\tau \sim N^{1+\nu}$  for the translocation time by comparison to the unimpeded motion of the polymer. Using FB [48] and LD [49, 51] models, a crossover from  $\tau \sim N^{2\nu}$  for relatively short polymers to  $\tau \sim N^{1+\nu}$  for longer chains was found in 2D. In 3D, we find that for faster translocation processes  $\tau \sim N^{1.37}$  [53, 54], while it crosses over to  $\tau \sim N^{1+\nu}$  for slower translocation, such as under weak driving forces and/or of high friction constants [55]. Moreover, using linear response theory with memory effects and some non-trivial assumptions, Vocks *et al.* [56] came up with an alternative estimate  $\tau \sim N^{\frac{1+2\nu}{1+\nu}}$  for 3D, which means  $\alpha = 1.37$  in 3D. Their  $\alpha$  in 3D is consistent with our numerical data for fast translocation, but fails to capture the scaling exponent for slow translocation.

However, above physical pictures are based on translocation into an unconfined *trans* side. Even for the case of an unconfined *trans* side, the translocated chain is highly compressed during the translocation process under fast translocation conditions [55], and thus even more severe nonequilibrium effects are expected under confinement. Quite little attention has been paid to the dynamics of translocation into confined environments. We here quantify the effects of the large entropic penalty on the confined chain and show that it significantly affects the translocation dynamics. In particular we find folded configurations of the confined chain on the *trans* side right after completion of the translocation process. Moreover we show that the force dependence of the translocation time significantly changes the  $1/F$  dependence for free translocation, and that the almost symmetric form of the

\*Author to whom the correspondence should be addressed; Electronic address: klu@ustc.edu.cn

†Electronic address: metz@ph.tum.de

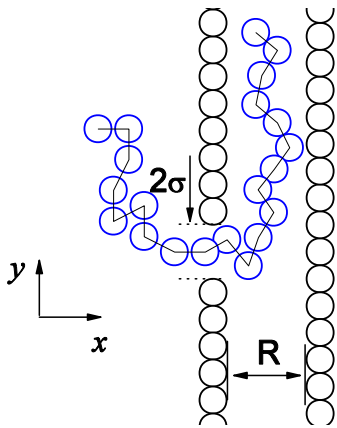


FIG. 1: (Color online) A schematic representation of polymer translocation through a pore into a 2D confined environment under an external driving force  $F$  across the pore. The pore width is  $2\sigma$ .

waiting time distribution turns over to a rapid increase throughout the translocation process. The paper is organized as follows. In section II, we briefly describe our model and the simulation technique. In section III, we present our results. Finally, we conclude in section IV.

## II. MODEL AND METHODS

In our numerical simulations, the polymer chains are modeled as bead-spring chains of Lennard-Jones (LJ) particles with the Finite Extension Nonlinear Elastic (FENE) potential. Excluded volume interaction between beads is modeled by a short range repulsive LJ potential:  $U_{LJ}(r) = 4\epsilon[(\frac{\sigma}{r})^{12} - (\frac{\sigma}{r})^6] + \epsilon$  for  $r \leq 2^{1/6}\sigma$  and 0 for  $r > 2^{1/6}\sigma$ . Here,  $\sigma$  is the diameter of a bead, and  $\epsilon$  is the depth of the potential. The connectivity between neighboring beads is modeled as a FENE spring with  $U_{FENE}(r) = -\frac{1}{2}kR_0^2 \ln(1 - r^2/R_0^2)$ , where  $r$  is the distance between consecutive beads,  $k$  is the spring constant and  $R_0$  is the maximum allowed separation between connected beads.

We consider a geometry as shown in Fig. 1, where two strips with separation  $R$  are formed by stationary particles within a distance  $\sigma$  from each other. One strip (“wall”) has a pore of diameter  $2\sigma$ . Between all bead-wall particle pairs, there exists the same short range repulsive LJ interaction as described above. In the Langevin dynamics simulation, each bead is subjected to conservative, frictional, and random forces, respectively, with [76]  $m\ddot{\mathbf{r}}_i = -\nabla(U_{LJ} + U_{FENE}) + \mathbf{F}_{\text{ext}} - \xi\mathbf{v}_i + \mathbf{F}_i^R$ . Here  $m$  is the bead’s mass,  $\xi$  is the friction coefficient,  $\mathbf{v}_i$  is the bead’s velocity, and  $\mathbf{F}_i^R$  is the random force which satisfies the fluctuation-dissipation theorem. The external force is expressed as  $\mathbf{F}_{\text{ext}} = F\hat{x}$ , where  $F$  is the external force strength exerted on the beads in the pore, and  $\hat{x}$  is a unit vector in the direction along the pore axis.

In the present work, the LJ parameters  $\epsilon$ ,  $\sigma$ , and  $m$

fix the system energy, length and mass units respectively, leading to the corresponding time scale  $t_{LJ} = (m\sigma^2/\epsilon)^{1/2}$  and force scale  $\epsilon/\sigma$ , which are of the order of ps and pN, respectively. The dimensionless parameters in the model are then chosen to be  $R_0 = 2$ ,  $k = 7$ ,  $\xi = 0.7$ , and  $F = 0.5 \dots 15$ .

In our model, each bead corresponds to a Kuhn length (twice of the persistence length) of a polymer. For a single-stranded DNA (ssDNA), the persistence length of the ssDNA is sequence and solvent dependent and varies in a wide range, to our knowledge, usually from about 1 to 4 nm. We assume the value of  $\sigma \sim 2.8$  nm for a ssDNA containing approximately four nucleotide bases. The average mass of a base in DNA is about 312 amu, so the bead mass  $m \approx 1248$  amu. We set  $k_B T = 1.2\epsilon$ , which means that the interaction strength  $\epsilon$  is  $3.39 \times 10^{-21}$  J at actual temperature 295 K. This leads to a time scale of 69.2 ps and a force scale of 1.2 pN. Each base (nucleotide) is estimated to have an effective charge of 0.094e from Ref. [9], leading to an effective charge of a bead with four bases of 0.376e. Thus, the voltage across the pore is between 28.1 and 843 mV for varying  $F$  from 0.5 to 15, within the range of experimental parameters [1–5].

The Langevin equation is then integrated in time by a method described by Ermak and Buckholz [77]. Initially, the first monomer of the chain is placed in the entrance of the pore, while the remaining monomers are under thermal collisions described by the Langevin thermostat to obtain an equilibrium configuration. Typically, we average our data over 1000 independent runs.

In Fig. 1, we assume that both ends of the channel are open. If that were not the case, such as for virus capsids, on the entering of the chain the fluid in the confined region would necessarily have to leave. To address such a problem it is therefore relevant to explicitly include the solvent in the model, which is beyond the scope of the present study.

## III. RESULTS AND DISCUSSION

Consider a polymer, such as DNA, confined to a nanochannel of width  $R$  with  $R$  being less than the radius of gyration of the molecule. The response of the polymer to confinement is primarily dictated by the relative value of  $R$  with respect to the chain persistence length. Depending on whether  $R$  is larger (de Gennes regime) or smaller (Odijk regime) than the chain persistence length, different scaling behaviors of the longitudinal size of the chain,  $R_{\parallel}$ , as a function of  $R$  were predicted in the pioneering theoretical studies by de Gennes [73] and Odijk [75], respectively. In the Odijk regime, the physics is dominated not by excluded volume but by the interplay of confinement and intrinsic polymer elasticity. In this work, we only consider the de Gennes regime, where the blob picture [73] is valid. To consider the Odijk regime, we would need to take into account the chain stiffness in the model. While this is certainly interesting we here

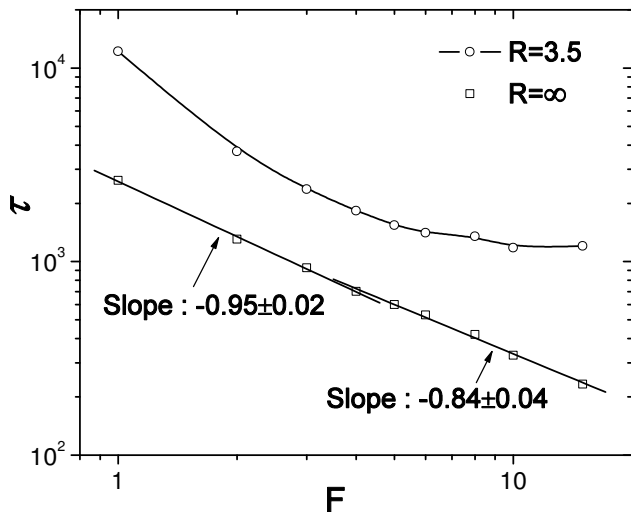


FIG. 2: Translocation time  $\tau$  as a function of  $F$  for  $R = 3.5$  and  $R = \infty$  in 2D. The chain length is  $N = 128$ .

focus on the polymeric aspects in the flexible chain limit.

According to the blob picture, for a polymer confined between two strips embedded in 2D the chain will extend along the channel forming blobs of size  $R$ . Each blob contains  $g = (R/\sigma)^{1/\nu_{2D}}$  monomers, where  $\nu_{2D}$  is the Flory exponent in 2D [73, 74], and the number of blobs is  $n_b = N/g = N(\sigma/R)^{1/\nu_{2D}}$ . Then, the blob picture predicts the longitudinal size of the chain to be  $R_{\parallel} \sim n_b R \sim N\sigma(\frac{\sigma}{R})^{1/\nu_{2D}-1} \sim NR^{-1/3}$  [73, 74]. The longitudinal relaxation time  $\tau_{\parallel}$  is defined as the time needed by a polymer to move a distance of the order of its longitudinal size,  $R_{\parallel}$ . Thus,  $\tau_{\parallel}$  scales as  $\tau_{\parallel} \sim \frac{R_{\parallel}^2}{\tilde{D}} \sim N^3 R^{-2/3}$ , with  $\tilde{D} = 1/N$  being the diffusion constant. The free energy cost in units of  $k_B T$  is  $\mathcal{F} = N(\sigma/R)^{1/\nu_{2D}}$ .

For polymer translocation into confined environments, a driving force is necessary to overcome the entropic repulsion  $f(R)$  exerted by already translocated monomers. Due to the highly non-equilibrium property of the translocation process, it is difficult to estimate the resisting force  $f(R)$ . If we assume that, for slow translocation processes, the resisting force  $f(R)$  scales as  $f(R) = CR^{\gamma}$ , with  $C$  and  $\gamma$  being the associated prefactor and the scaling exponent, respectively; then, under an external driving force  $F$  in the pore the translocation time  $\tau$  can be written as  $\tau \sim \frac{N^{\alpha}}{F-f(R)} \sim \frac{N^{\alpha}}{F(1-CR^{\gamma}/F)}$  with  $\alpha$  being the scaling exponent of  $\tau$  with chain length  $N$ . Due to  $\tau_{\infty} \sim \frac{N^{\alpha}}{F}$  for an unconfined system with  $R \sim \infty$ , we have  $1 - \frac{\tau_{\infty}}{\tau} \sim CR^{\gamma}/F$ . Based on this relationship, we examine the dependence of  $\tau$  on  $R$ .

#### A. Translocation time as a function of the driving force

As shown in Fig. 2 for unconfined system  $R = \infty$ , the dependence of  $\tau$  on the driving force scales as  $F^{-1}$

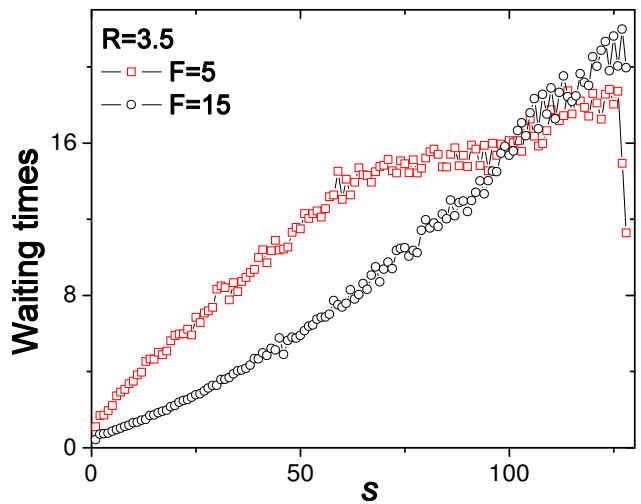


FIG. 3: (Color online) Waiting time distribution for  $N = 128$  and  $R = 3.5$  under different  $F$ . The waiting time of monomer  $s$  is defined as the average time between the events that monomer  $s$  and monomer  $s + 1$  exit the pore.

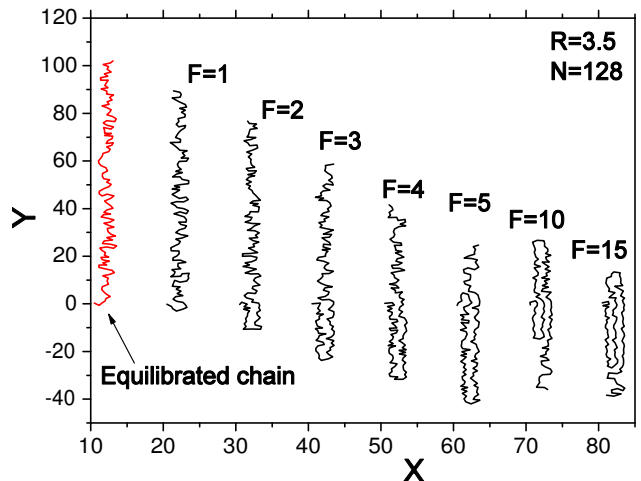


FIG. 4: (Color online) Typical chain conformation at the moment just after translocation for  $N = 128$  and  $R = 3.5$  under different  $F$ .

for weak driving forces  $F \leq 4$ . This simple scaling behavior can be understood by considering the steady state motion of the polymer through the nanopore. The average velocity is determined by balancing the frictional damping force (proportional to the velocity) with the external driving force. This leads to an average velocity proportional to the driving force  $F$ , and hence a translocation time  $\tau \sim F^{-1}$ . For  $F > 4$ ,  $\tau \sim F^{-0.84}$  due to a pronounced non-equilibrium situation where the chain is highly distorted, as illustrated in our previous work [55]. For this case, only part of the chain on the *cis* side can respond immediately, while the remaining part near the chain end does not feel the force yet. As a result, a part of the chain on the *cis* side is deformed to a trumpet and even stem-and-flower shape, while the translocated por-

tion on the *trans* side has a compact spherical shape, as it does not have time to diffuse away from the pore exit. In a recent theoretical study [59], the effect of a trumpet shape of the chain on the *cis* side, on the translocation dynamics was found to cause a breakdown of the  $\tau \sim F^{-1}$  scaling. However, this theory neglects effects due to the compacted chain structure on the *trans* side.

However, for confined systems the effect of the driving force on the translocation time is completely different, as shown in Fig. 2 for  $R = 3.5$ . With increasing  $F$ , the translocation time initially decreases rapidly, and then almost saturates for  $F \geq 10$ . As noted above,  $\tau \sim \frac{N^\alpha}{F(1-CR^\gamma/F)}$  for an equilibrium process. With decreasing  $F$ , the resisting force  $f(R)$  is more and more important and it slows down translocation. This is the reason why the initial slope is faster than that for translocation into a free *trans* side. With increasing  $F$ ,  $f(R)$  becomes important again, which indicates that the resisting force  $f(R)$  induced by crowding effects from already translocated monomers plays an important role in the observed behavior.

To further understand this behavior, we examine the dynamics of a single segment passing through the pore during translocation. The nonequilibrium nature of translocation has a significant effect on it. We have numerically calculated the waiting times for all monomers in a chain of length  $N$ . We define the waiting time of monomer  $s$  as the average time between the events that monomer  $s$  and monomer  $s + 1$  exit the pore. In our previous work, we found that the waiting time depends strongly on the monomer positions in the chain under the driving force  $F = 5$  [48, 49]. For relatively short polymers, such as  $N = 100$ , the monomers in the middle of the polymer need the longest time to translocate and the distribution is close to symmetric. In contrast, for the confined system with  $R = 3.5$  and  $N = 128$ , we find a slow increase after the monomers in the middle of the polymer (i.e., beyond  $s = N/2$ ) and a further, more rapid increase after  $s \approx 100$  for  $F = 5$ , see Fig. 3. Increasing the driving force further to  $F = 15$ , the waiting time rapidly increases throughout. Moreover, it takes longer for monomers at  $s > 100$  to exit the pore for strong driving force  $F = 15$  than that for  $F = 5$ . These results indicate that during later stages of translocation the high density of segments in the channel slows down the translocation and the inverse proportionality  $\tau \sim F^{-1}$  breaks down. Especially for strong driving forces the crowding effect is more pronounced, leading to almost the same translocation time for  $F = 10$  and  $F = 15$ . These results are different from translocation into two parallel walls (3D), where we observed a relatively fast turnover between the scaling  $\tau \sim F^{-1.25}$  at weak forces and the behavior  $\tau \sim F^{-0.8}$  at strong forces [78].

Fig. 4 shows the typical chain conformation at the moment just after translocation for  $N = 128$  and  $R = 3.5$  under different  $F$ . Compared with the equilibrated chain, the chains become more compressed with increasing  $F$ .

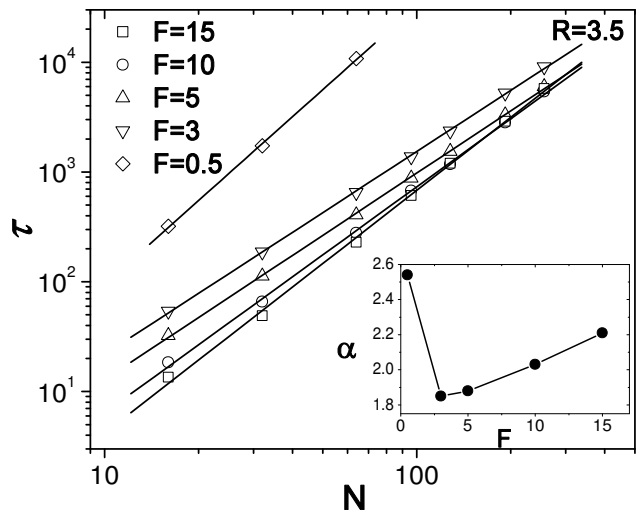


FIG. 5: Translocation time  $\tau$  as a function of the chain length  $N$  for  $R = 3.5$  and different  $F$  in 2D. The insert shows the scaling exponent  $\alpha$  of  $\tau$  with  $N$  for different driving forces  $F$ . For  $F=0.5, 3, 5, 10$  and  $15$ ,  $\alpha = 2.54 \pm 0.04, 1.85 \pm 0.01, 1.88 \pm 0.01, 2.03 \pm 0.02$ , and  $2.21 \pm 0.04$ , respectively.

In particular, a folding of the chain is observed for  $F \geq 2$ , reflecting stronger resisting forces with increasing  $F$ . At  $F \geq 10$  there even occur triple layers in the chain configuration. As can be seen the chains in this folded state are almost entirely devoid of the larger-amplitude undulations observed in the equilibrium configuration. This also provides a way to induce chain folding by driving polymers into unidimensionally confined environments such as small channels.

We stop to note that here we confine the analysis to the variation of the driving force  $F$ . As demonstrated in Ref. [55] the variation of the friction coefficient  $\xi$  has a similar effect.

## B. Translocation time as a function of the chain length

Previously [48, 49, 51], we investigated the polymer translocation into an unconfined *trans* side ( $R = \infty$ ) under an external driving force  $F = 5$  in the pore. Both the 2D fluctuating bond model with single Monte Carlo moves [48] and Langevin [49, 51] simulations show  $\tau \sim N^{2\nu} \sim N^{1.5}$  for relatively short chains  $N \leq 200$ .

However, for polymer translocation into the region between two strips, the dynamics is completely different. As shown in Fig. 5, for the same driving force  $F = 5$  for  $R = 3.5$ , we find  $\tau \sim N^{1.88 \pm 0.01}$  and translocation velocity  $v \sim N^{1.08 \pm 0.02}$  close to the inversely linear scaling  $v \sim N^{-1}$ . During the translocation process, the chain moves a distance of  $R_g + R_{\parallel}$  instead of  $2R_g$  for an unconfined system, where  $R_{\parallel}$  is the longitudinal size of the chain. For a polymer confined between two strips embedded in 2D, the longitudinal size of the

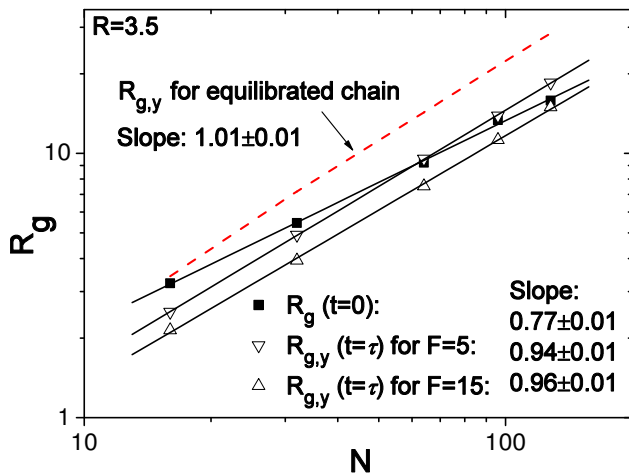


FIG. 6: (Color online) The radius of gyration of the chain before translocation and at the moment just after the translocation for  $R = 3.5$  and different  $F$ . Here, the  $x$  direction is perpendicular to the wall, and  $y$  is the direction along the wall.

chain is  $R_{\parallel} \sim N$  (see above scaling results from the blob picture), which is the dominant term over the second term,  $R_g \sim N^{\nu_{2D}}$ . Thus, the translocation time roughly scales as  $\tau \sim \frac{R_{\parallel}}{v} \sim N^2$ . Decreasing the driving force to  $F = 3.0$ , the scaling exponent almost does not change,  $\tau \sim N^{1.85 \pm 0.01}$ . Decreasing the driving force further to  $F = 0.5$ , we find the translocation dynamics crosses over to another regime with  $\alpha = 2.54 \pm 0.04$  at least for  $N \leq 64$ , which is still lower than the expected scaling exponent 3.0 of the relaxation time as a function of the chain length for a chain in a narrow channel. Due to expensive computation, we cannot access cases with longer chains and/or weaker driving forces. Increasing the driving force  $F$  from 5 to 10 and 15, we find  $\tau \sim N^{2.03 \pm 0.02}$  and  $\tau \sim N^{2.21 \pm 0.04}$ , respectively. This is, however, an a priori unexpected increase of  $\alpha$  with increasing  $F$ , which indicates that the translocation is slowed down for strong driving forces. Particularly, for  $N = 256$  the translocation time almost does not change for  $F = 5, 10$  and  $15$ , due to the formation of a folded chain conformation.

Altogether, compared with an unconfined environment we observe the nonuniversal dependence of the translocation time  $\tau$  on the chain length  $N$ . Particularly, there is a minimum of  $\alpha$  as a function of  $F$ , as shown in the insert of the Fig. 5, due to the more severe crowding effect for stronger driving forces. The scaling exponent does not change for  $F = 15$  compared with  $F = 5$ . These results are different from the translocation into two parallel walls (3D) with the same  $R$ , where for weak driving forces  $\tau$  scales exactly in the same manner as the chain relaxation time and crosses over to exponent 1.37 for strong driving forces [78]. As intuitively expected, these observations demonstrate that confinement effects are more relevant in the 1D channel configuration compared to the 2D confinement of the chain sandwiched between two parallel

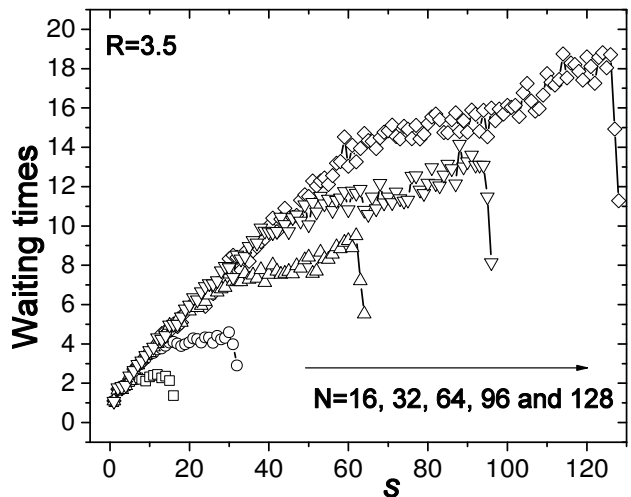


FIG. 7: Waiting time distribution for different  $N$  under the driving force  $F = 5$  and  $R = 3.5$ .

walls.

Fig. 6 shows the radius of gyration of the chain before the translocation and at the moment just after the translocation for  $R = 3.5$  and different  $F$ . Just after the translocation, the chains are compressed in the  $y$  direction compared with the equilibrated chain. However, the scaling exponent of  $R_{g,y} \sim N$  almost does not change even for  $F = 15$ . Fig. 7 shows the waiting time distribution for different chain lengths for  $F = 5.0$  and  $R = 3.5$ . Similar distributions are observed for different chain length. This behavior reflects the crowding effect of partially translocated monomers, which greatly slows down translocation.

### C. Translocation time as a function of the channel width $R$

As shown in Fig. 8, there exist two regimes in the behavior of  $\tau$  as a function of  $R$  for  $F = 5.0$  and  $N = 128$ .  $\tau$  decreases rapidly with increasing  $R$  and then almost saturates for larger  $R$ . The insert of Fig. 8 shows  $1 - \frac{\tau}{\tau_0}$  as a function of  $R$ . For  $R \leq 6$ , we find the exponent  $\gamma = -1.06 \pm 0.07$ . For equilibrium translocation process  $f(R) \sim R^{-1/\nu_{2D}}$ , which gives the exponent  $-1/\nu_{2D} = -1.33$ . The numerical exponent 1.06 does not agree with this result, which indicates that the translocation is a highly non-equilibrium process.

Fig. 9 shows the radius of gyration of the chain before translocation and at the moment just after the translocation for  $N = 128$  and  $F = 5$  versus the channel size  $R$ . Just after the translocation, the chains are highly compressed along the channel and  $R_{g,y} \sim R^{-0.92}$  for  $R \leq 5$  compared with the equilibrated chains, where  $R_{g,y} \sim R^{-0.37}$  as predicted.

Fig. 10 depicts the waiting time distribution for different  $R$ . For larger  $R$ , we observe a symmetric distribution

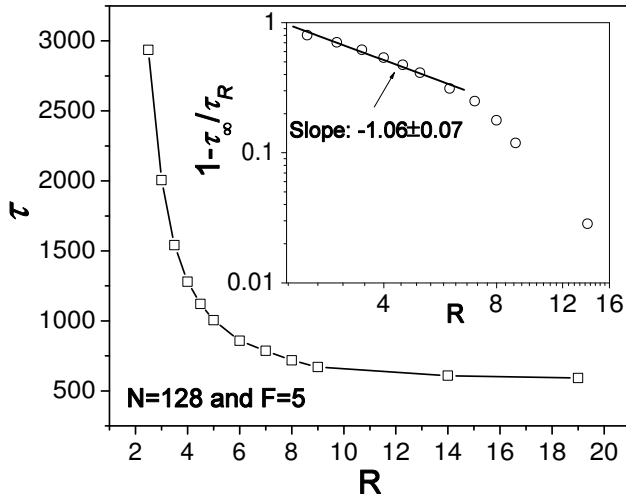


FIG. 8: Translocation time  $\tau$  as a function of  $R$  for chain length  $N = 128$  under the driving force  $F = 5$ .

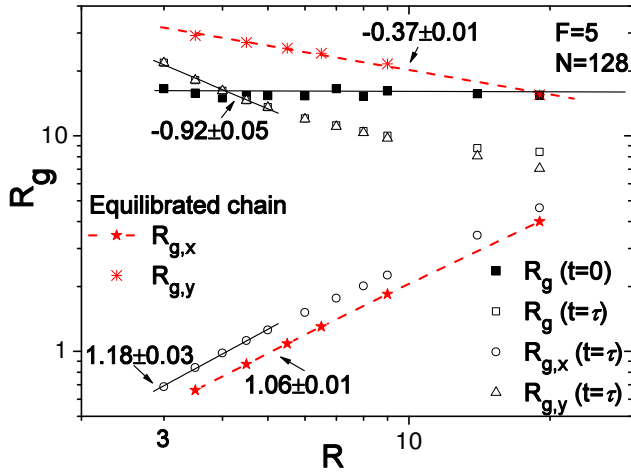


FIG. 9: (Color online) The radius of gyration of the chain before translocation and at the moment just after the translocation for  $N = 128$ ,  $F = 5$  versus the channel size  $R$ . Here, the  $x$  direction is perpendicular to the wall, and  $y$  is the direction along the wall.

with respect to the middle monomer  $s = N/2$  [48, 49]. With decreasing  $R$ , the waiting times increase. Particularly, it takes much longer time for monomers  $s > N/2$  to exit the pore. For  $R = 5$ , the waiting times approximately saturate after  $s > N/2$ , while they continuously increase for  $R \leq 4$ . This behavior is due to the crowding of the translocated monomers. As to the first moment of the translocation coordinate  $\langle s(t) \rangle \sim t^\beta$ , previous results [53] show  $\beta \approx 1/\alpha = 0.67$  with  $\alpha \approx 2\nu = 1.50$  for  $R = \infty$ . Fig. 11 shows  $\langle s(t) \rangle \sim t^\beta$  for  $N = 128$  and  $F = 5$  for different  $R$ . For  $R = \infty$ ,  $\beta = 0.70 \pm 0.01$  as expected and it continuously decreases to  $0.58 \pm 0.01$  for  $R = 3$ . Here,  $\beta < 1$  is a signature of anomalous diffusion [79]. The values of  $\beta$  in Fig. 11 imply that the scaling exponent  $\alpha$  can change from  $\approx 2\nu$  to  $\approx 2$ , depending on

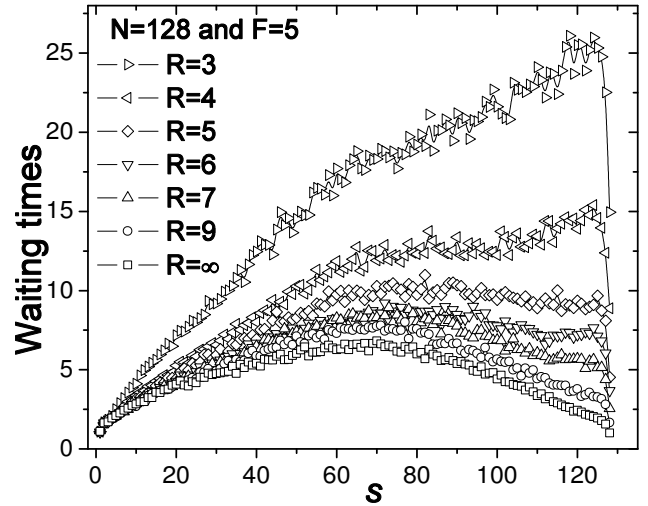


FIG. 10: Waiting time distribution for different  $R$ . The chain length  $N = 128$  and the driving force  $F = 5$ .

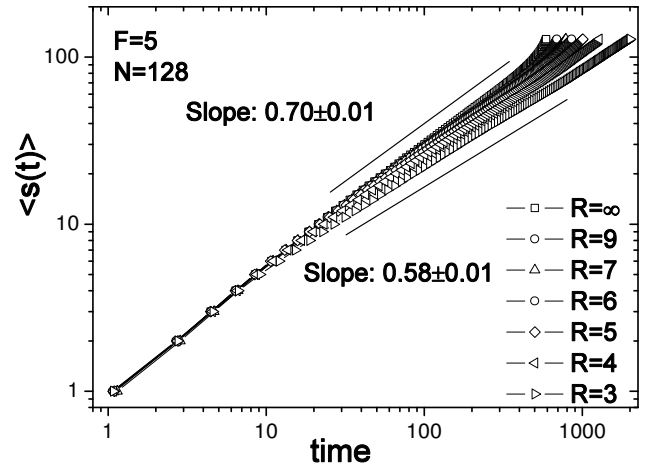


FIG. 11: The number of translocated monomers as a function of time,  $\langle s(t) \rangle$ , for different  $R$ . The chain length  $N = 128$  and the driving force  $F = 5$ .

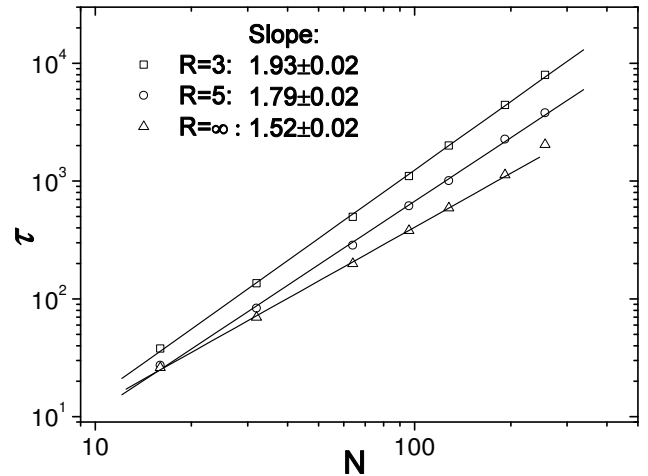


FIG. 12: Translocation time as a function of the chain length for different  $R$ . The driving force  $F = 5$ .

$R$  due to highly non-equilibrium effects. This is clearly indicated in Fig. 12, where  $\alpha = 1.52 \pm 0.02$ ,  $1.79 \pm 0.02$  and  $1.93 \pm 0.02$  for  $R = \infty$ , 5 and 3, respectively.

#### IV. CONCLUSIONS

Using two-dimensional Langevin dynamics simulations, we investigated the dynamics of polymer translocation into a narrow channel of width  $R$  through a nanopore under a driving force  $F$ . Due to the crowding effect induced by the partially translocated monomers, the translocation dynamics is greatly changed compared with an unconfined environment. Namely we observe a nonuniversal dependence of the translocation time  $\tau$  on the chain length  $N$ :  $\tau$  initially decreases rapidly and then saturates with increasing  $R$ , and, moreover, an  $R$  dependence of the scaling exponent  $\alpha$  in the law  $\tau \sim N^\alpha$  is observed. The inversely linear scaling of  $\tau$  with  $F$  breaks down and we observe a minimum of  $\alpha$  as a function of  $F$ . These behaviors are clearly interpreted in terms of the waiting time of an individual segment for passing through the pore during translocation, as well as in terms of statistical quantities such as the width of the chain. In particular we observe folded configurations of the chain

in the channel, at high driving forces even a structure with a double-fold exists. Similar effects of nonequilibrium nature are expected in biological cells. There, the passage of a translocating chain is opposed by a crowded environment in which larger biomolecules occupy more than 40% of the volume [80, 81].

Our findings are of interest from a purely polymer physics point of view, contributing to a more complete picture of polymer translocation through a narrow pore, once more pronouncing the importance to consider nonequilibrium situations. A direct application of our findings may be of relevance for parallel fluidic channel setups consisting of stacked parallel slices. In each slice the chain initially is in an unconfined two-dimensional conformation, before being forced through the pore into the effectively 1D channel.

#### Acknowledgments

K. L. acknowledges the support from the University of Science and Technology of China through its startup funding of CAS Bairen Program. This work has been supported in part by the Deutsche Forschungsgemeinschaft (DFG).

- 
- [1] J. J. Kasianowicz, E. Brandin, D. Branton and D. W. Deamer, *Proc. Natl. Acad. Sci. U.S.A.* **93**, 13770 (1996).
  - [2] A. Meller, *J. Phys.: Condens. Matter* **15**, R581 (2003).
  - [3] A. Meller, L. Nivon, E. Brandin, J. A. Golovchenko, and D. Branton, *Proc. Natl. Acad. Sci. U.S.A.* **97**, 1079 (2000).
  - [4] A. Meller, L. Nivon, and D. Branton, *Phys. Rev. Lett.* **86**, 3435 (2001).
  - [5] A. Meller and D. Branton, *Electrophoresis* **23**, 2583 (2002).
  - [6] M. Akeson, D. Branton, J. J. Kasianowicz, E. Brandin, and D. W. Deamer, *Biophys. J.* **77**, 3227 (1999).
  - [7] M. Wanunu and A. Meller, *Nano Lett.* **7**, 1580 (2007).
  - [8] S. M. Iqbal, D. Akin, and R. Bashir, *Nat. Nanotech.* **2**, 243 (2007).
  - [9] A. F. Sauer-Budge, J. A. Nyamwanda, D. K. Lubensky, and D. Branton, *Phys. Rev. Lett.* **90**, 238101 (2003).
  - [10] J. Mathe, H. Visram, V. Viasnoff, Y. Rabin, and A. Meller, *Biophys. J.* **87**, 3205 (2004).
  - [11] S. E. Henrickson, M. Misakian, B. Robertson, and J. J. Kasianowicz, *Phys. Rev. Lett.* **85**, 3057 (2000).
  - [12] J. J. Kasianowicz, S. E. Henrickson, H. H. Weetall, and B. Robertson, *Anal. Chem.* **73**, 2268 (2001).
  - [13] J. J. Kasianowicz, J. W. F. Robertson, E. R. Chan, J. E. Reiner, and V. M. Standford, *Annu. Rev. Anal. Chem.* **1**, 737 (2008).
  - [14] V. M. Standford, and J. J. Kasianowicz, *IEEE workshop on genomic signal processing and statistics* (May 26, 2004, Baltimore, Maryland).
  - [15] J. W. F. Robertson, C. G. Rodrigues, V. M. Standford, K. A. Rubinson, O. V. Krasilnikov, and J. J. Kasianowicz, *Proc. Natl. Acad. Sci. U.S.A.* **104**, 8207 (2007).
  - [16] J. L. Li, D. Stein, C. McMullan, D. Branton, M. J. Aziz, and J. A. Golovchenko, *Nature* (London) **412**, 166 (2001).
  - [17] J. L. Li, M. Gershow, D. Stein, E. Brandin, and J. A. Golovchenko, *Nat. Mater.* **2**, 611 (2003).
  - [18] D. Fologea, J. Uplinger, B. Thomas, D. S. McNabb, and J. L. Li, *Nano Lett.* **5**, 1734 (2005).
  - [19] U. F. Keyser, J. B. M. Koelman, S. van Dorp, D. Krapf, R. M. M. Smeets, S. G. Lemay, N. H. Dekker, and C. Dekker, *Nat. Phys.* **2**, 473 (2006).
  - [20] U. F. Keyser, J. van der Does, C. Dekker, and N. H. Dekker, *Rev. Sci. Instr.*, **77**, 105105 (2006).
  - [21] C. Dekker, *Nat. Nanotech.* **2**, 209 (2007).
  - [22] E. H. Trepagnier, A. Radenovic, D. Sivak, P. Geissler, and J. Liphardt, *Nano Lett.* **7**, 2824 (2007).
  - [23] A. J. Storm, J. H. Chen, X. S. Ling, H. W. Zandbergen, and C. Dekker, *Nat. Mater.* **2**, 537 (2003).
  - [24] A. J. Storm, J. H. Chen, H. W. Zandbergen, and C. Dekker, *Phys. Rev. E* **71**, 051903 (2005).
  - [25] A. J. Storm, C. Storm, J. Chen, H. Zandbergen, J. -F. Joanny and C. Dekker, *Nano Lett.* **5**, 1193 (2005).
  - [26] S. M. Simon, C. S. Peskin, and G. F. Oster, *Proc. Natl. Acad. Sci. U.S.A.* **89**, 3770 (1992).
  - [27] W. Sung and P. J. Park, *Phys. Rev. Lett.* **77**, 783 (1996).
  - [28] P. J. Park and W. Sung, *J. Chem. Phys.* **108**, 3013 (1998).
  - [29] E. A. diMarzio and A. L. Mandell, *J. Chem. Phys.* **107**, 5510 (1997).
  - [30] M. Muthukumar, *J. Chem. Phys.* **111**, 10371 (1999).
  - [31] M. Muthukumar, *J. Chem. Phys.* **118**, 5174 (2003).
  - [32] C. Y. Kong and M. Muthukumar, *Electrophoresis* **23**, 2697 (2002); C. Y. Kong and M. Muthukumar, *J. Chem.*

- Phys.* **120**, 3460 (2004); C. Y. Kong and M. Muthukumar, *J. Am. Chem. Soc.* **127**, 18252 (2005); M. Muthukumar and C. Y. Kong, *Proc. Natl. Acad. Sci. U.S.A.* **103**, 5273 (2006); C. Forrey and Muthukumar, *J. Chem. Phys.* **127**, 015102 (2007); C. T. A. Wong and M. Muthukumar, *J. Chem. Phys.* **128**, 154903 (2008).
- [33] D. K. Lubensky and D. R. Nelson, *Biophys. J.* **77**, 1824 (1999).
- [34] Y. Kafri, D. K. Lubensky, and D. R. Nelson, *Biophys. J.* **86**, 3373 (2004).
- [35] E. Slonkina and A. B. Kolomeisky, *J. Chem. Phys.* **118**, 7112 (2003); S. Kotsev and A. B. Kolomeisky, *J. Chem. Phys.* **125**, 084906 (2006); A. Mohan, A. B. Kolomeisky and M. Pasquali, *J. Chem. Phys.* **128**, 125104 (2008).
- [36] S. Matysiak, A. Montesi, M. Pasquali, A. B. Kolomeisky, and C. Clementi, *Phys. Rev. Lett.* **96**, 118103 (2006).
- [37] T. Ambjornsson, S. P. Apell, Z. Konkoli, E. A. DiMarzio, and J. J. Kasianowicz, *J. Chem. Phys.* **117**, 4063 (2002).
- [38] R. Metzler and J. Klafter, *Biophys. J.* **85**, 2776 (2003).
- [39] T. Ambjornsson and R. Metzler, *Phys. Biol.* **1**, 19 (2004).
- [40] T. Ambjornsson, M. A. Lomholt, and R. Metzler, *J. Phys.: Condens. Matter* **17**, S3945 (2005).
- [41] A. Baumgartner and J. Skolnick, *Phys. Rev. Lett.* **74**, 2142 (1995).
- [42] J. Chuang, Y. Kantor and M. Kardar, *Phys. Rev. E* **65**, 011802 (2001).
- [43] Y. Kantor and M. Kardar, *Phys. Rev. E* **69**, 021806 (2004).
- [44] J. L. A. Dubbeldam, A. Milchev, V.G. Rostiashvili, and T.A. Vilgis, *Phys. Rev. E* **76**, 010801(R) (2007).
- [45] J. L. A. Dubbeldam, A. Milchev, V.G. Rostiashvili, and T.A. Vilgis, *Europhys. Lett.* **79**, 18002 (2007).
- [46] A. Milchev, K. Binder, and A. Bhattacharya, *J. Chem. Phys.* **121**, 6042 (2004).
- [47] K. Luo, T. Ala-Nissila, and S. C. Ying, *J. Chem. Phys.* **124**, 034714 (2006).
- [48] K. Luo, I. Huopaniemi, T. Ala-Nissila, and S. C. Ying, *J. Chem. Phys.* **124**, 114704 (2006).
- [49] I. Huopaniemi, K. F. Luo, T. Ala-Nissila, and S. C. Ying, *J. Chem. Phys.* **125**, 124901 (2006).
- [50] I. Huopaniemi, K. F. Luo, T. Ala-Nissila, and S. C. Ying, *Phys. Rev. E* **75**, 061912 (2007); S. T. T. Ollila, K. Luo, T. Ala-Nissila, S. C. Ying, *Eur. Phys. J. E* **28**, 385 (2009).
- [51] K. Luo, T. Ala-Nissila, S. C. Ying, and A. Bhattacharya, *J. Chem. Phys.* **126**, 145101 (2007).
- [52] K. Luo, T. Ala-Nissila, S. C. Ying, and A. Bhattacharya, *Phys. Rev. Lett.* **99**, 148102 (2007); **100**, 058101 (2008); *Phys. Rev. E* **78**, 061911 (2008); **78**, 061918 (2008).
- [53] K. Luo, S. T. T. Ollila, I. Huopaniemi, T. Ala-Nissila, P. Pomorski, M. Karttunen, S. C. Ying, and A. Bhattacharya, *Phys. Rev. E* **78**, 050901(R)(2008).
- [54] K. Luo, R. Metzler, T. Ala-Nissila, S. C. Ying, *Phys. Rev. E* **80**, 021907 (2009).
- [55] K. Luo, T. Ala-Nissila, S. C. Ying, and R. Metzler, *EPL* **88**, 68006 (2009).
- [56] H. Vocks, D. Panja, G. T. Barkema, and R. C. Ball, *J. Phys.: Condens. Matter* **20**, 095224 (2008).
- [57] A. Bhattacharya, W. H. Morrison, K. Luo, T. Ala-Nissila, S. C. Ying, A. Milchev, and K. Binder, *Eur. Phys. J. E* **29**, 423 (2009); A. Bhattacharya and K. Binder, *Phys. Rev. E* **81**, 041804(2010).
- [58] S. Guillouzie and G. W. Slater, *Phys. Lett. A* **359**, 261 (2006); M. G. Gauthier and G. W. Slater, *Eur. Phys. J. E* **25**, 17 (2008); M. G. Gauthier and G. W. Slater, *J. Chem. Phys.* **128**, 065103 (2008).
- [59] T. Sakaue, *Phys. Rev. E* **76**, 021803(2007); **81**, 041808 (2010).
- [60] S.-S. Chern, A. E. Cardenas, and R. D. Coalson, *J. Chem. Phys.* **115**, 7772 (2001).
- [61] H. C. Loebel, R. Randel, S. P. Goodwin, and C. C. Matthai, *Phys. Rev. E* **67**, 041913 (2003).
- [62] R. Randel, H. C. Loebel, and C. C. Matthai, *Macromol. Theory Simul.* **13**, 387 (2004).
- [63] Y. Lansac, P. K. Maiti, and M. A. Glaser, *Polymer* **45**, 3099 (2004).
- [64] Z. Farkas, I. Derenyi, and T. Vicsek, *J. Phys.: Condens. Matter* **15**, S1767 (2003).
- [65] P. Tian and G. D. Smith, *J. Chem. Phys.* **119**, 11475 (2003).
- [66] Y. D. He, H. J. Qian, Z. Y. Lu, and Z. S. Li, *Polymer* **48**, 3601 (2007); Y. C. Chen, C. Wang, and M. Luo, *J. Chem. Phys.* **127**, 044904 (2007); Y. J. Xie, H. Y. Yang, H. T. Yu, Q. W. Shi, X. P. Wang, and J. Chen, *J. Chem. Phys.* **124**, 174906 (2006); C. Chen, L. Teng, and H. J. Liang, *Chin. J. Chem. Phys.* **21**, 275 (2008); M. B. Luo, *Polymer* **48**, 7679 (2007); Z. Y. Yang, Z. Q. Pan, L. X. Zhang, and H. J. Liang, *Polymer* **51**, 2795 (2010).
- [67] D. Wei, W. Yang, X. Jin, and Q. Liao, *J. Chem. Phys.* **126**, 204901 (2007).
- [68] R. Zandi, D. Reguera, J. Rudnick, and W. M. Gelbart, *Proc. Natl. Acad. Sci. U.S.A.* **100**, 8649 (2003).
- [69] S. Tsuchiya and A. Matsuyama, *Phys. Rev. E* **76**, 011801 (2007).
- [70] S. Kotsev and A. B. Kolomeisky, *J. Chem. Phys.* **125**, 084906 (2006).
- [71] U. Bockelmann, and V. Viasnoff, *Biophys. J.* **94**, 2716 (2008).
- [72] H. A. Kramers, *Physica* **7**, 284 (1940).
- [73] P. G. de Gennes, *Scaling Concepts in Polymer Physics* (Cornell University Press, Ithaca, NY, 1979).
- [74] M. Rubinstein, and R. Colby, *Polymer Physics* (Oxford University Press, Oxford, 2003).
- [75] T. Odijk, *Macromolecules* **16**, 1340 (1983).
- [76] M.P. Allen, D.J. Tildesley, *Computer Simulation of Liquids* (Oxford University Press, 1987).
- [77] D. L. Ermak and H. Buckholz, *J. Comput. Phys.* **35**, 169 (1980).
- [78] K. Luo and R. Metzler, *J. Chem. Phys.*, in press.
- [79] R. Metzler and J. Klafter, *Phys. Rep.* **339**, 1 (2000); *J. Phys. A* **37**, R161 (2004).
- [80] J. A. Dix, and A. S. Verkman, *Annu. Rev. Biophys.* **37**, 247 (2008); H. X. Zhou, G. Rivas, and A. P. Minton, *ibid* **37**, 375 (2008).
- [81] D. E. Smith, S. J. Tans, S. B. Smith, S. Grimes, D. E. Anderson, and C. Bustamante, *Nature* **413**, 748 (2001); I. Ali, D. Marenduzzo, and J. M. Yeomans, *J. Chem. phys.* **121**, 8635 (2004).